Results in Physics 13 (2019) 102156

Contents lists available at ScienceDirect

Results in Physics

journal homepage: www.elsevier.com/locate/rinp

Physical properties of high-strength bolt materials at elevated temperatures

Xiao-Ping Pang[a,b,c], Ying Hu[a,b,*], Sheng-Lin Tang[a,b], Zheng Xiang[a,b], Guilin Wu[d], Tanchumin Xu[e], Xing-Qiang Wang[f,g]

[a] Key Laboratory of New Technology for Construction of Cities in Mountain Areas (Chongqing University), Ministry of Education, Chongqing 400045, PR China
[b] School of Civil Engineering, Chongqing University, Chongqing 400045, PR China
[c] College of Mechanical Engineering, Chongqing University, No. 174 Sha Zheng Street, Shapingba District, Chongqing 400044, PR China
[d] College of Materials Science and Engineering, Chongqing University, Chongqing 400044, PR China
[e] School of Mathematical Sciences, Beijing Normal University, Beijing, PR China
[f] Centre for Infrastructure Engineering, Western Sydney University, Penrith, NSW 2751, Australia
[g] Department of Civil Engineering, Shandong Polytechnic, Jinan, Shandong Province 250104, PR China

ARTICLE INFO

Keywords:
High-strength
Bolt
Fire
Reduction
Elevated-temperature
Stress
Strain
Carbon steel

ABSTRACT

Carbon steel bolts have been broadly utilized in modern building construction. Fire performance of these components has been investigated in the published journals aiming at deriving their reduction factors at elevated temperatures. However, it should be noted that materials employed for manufacturing high-strength structural bolts may be different from country to country. Meanwhile, the present research efforts mainly focused on fire performance of carbon steel bolts instead of their material properties. Therefore, this paper developed an experimental program for investigation of the elevated-temperature material properties for three types of high-strength bolts with property classes 8.8, 10.9 and 12.9. Standard coupon specimens were milled from carbon steel bolts. The temperatures of tensile testing were in the range of 20–900 °C. The key material properties were extracted from the recorded stress–strain curves. These tested results were compared with those of high-strength bolts and steels from the literature. It was found that different materials for bolt making has a negligible influence on the deterioration of material properties at elevated temperatures, not including strains (ε_u and ε_f). In contrast, the strength reduction was generally faster than the majority of high-strength steels at elevated temperatures (over 300 °C). In addition, the analytical models were proposed for describing the deterioration of yield strength (f_{yT}), Young's modulus (E_{sT}), ultimate strain (ε_{uT}) and fracture strain (ε_{fT}) at elevated temperatures.

Introduction

High-strength structural bolts are normally responsible for transferring loading from structural beams to columns in a bolted connection, contributing to stability and integrity of a structural system and withstanding both thermal and mechanically induced loads produced from a catastrophic event such as fire [1,2]. In application, ISO committee and Chinese standards recommended three types of high-strength structural bolts for building construction with basic requirements on mechanical properties and tolerances in the geometrical details. Furthermore, a single structural bolt may receive both tensile and shear forces simultaneously in a bolted connection. Its failure might be caused by bolt fracture or threads stripping-off, which has already been confirmed in the previous publications [1,3,4].

Even though most of structural bolts are failed by bolt fracture (material failure), we still observed some of them failed due to the looser degree of fit between internal and external threads. This phenomenon is well known as threads stripping caused by threads overtapping, leading to 20% reduction of bolt capacity accordingly [3,4]. Another important aspect is thread engagement length. The observation shows that increasing the height of nut may reduce the probability of threads stripping (thread failure) [5]. As indicated, this failure mechanism is less ductile than bolt fracture and is therefore generally not expected in connection design. Meanwhile, fire resistance of a steel-framed structure would be seriously influenced by this mechanism of failure. Although failure of structural bolts is very complicated in a fire or post-fire situation, understanding its materials is a fundamental element for better understanding the performance of bolted

* Corresponding author at: Key Laboratory of New Technology for Construction of Cities in Mountain Areas (Chongqing University), Ministry of Education, Chongqing 400045, PR China. School of Civil Engineering, Chongqing University, Chongqing 400045, PR China.
E-mail address: y.hu@cqu.edu.cn (Y. Hu).

https://doi.org/10.1016/j.rinp.2019.102156
Received 7 November 2018; Received in revised form 26 February 2019; Accepted 26 February 2019
Available online 09 March 2019

Notation

E_s	elastic modulus at room temperature
E_{sT}	elastic modulus at high temperature T (°C)
f_y	0.2% yield strength at room temperature
f_{yT}	0.2% yield strength at high temperature T (°C)
f_u	ultimate strength at room temperature
f_{uT}	ultimate strength at high temperature T (°C)
ε_u	strain at ultimate strength at room temperature
ε_{uT}	strain at ultimate strength at high temperature T (°C)
ε_f	strain at fracture at room temperature
ε_{fT}	strain at fracture at high temperature T (°C)
T	specified temperature

connections.

On the basis of ISO 898-1 [6], two types of materials: carbon steels and alloy steels, are commonly provided for production of structural bolts. Moreover, it is very common for carbon steels to have additives like Boron, Mn and Cr for enhancement of their material strength and hardenability. These materials are commonly forged into steel wires or steel rods (steel bars) with determined dimensions before manufacturing. Then structural bolts are manufactured through a number of successive mechanical processes, including stretching, drawing, cutting, head forming and thread rolling [7]. The final quenching and tempering process is only for achieving the desired material properties. In other words, the material properties of high-strength structural bolts are due to a consequence of combination of chemical compositions and manufacturing processes (including heat treatment). Meanwhile, it should be noticed that the mechanism of bolt fracture shall be attributed to the failure of materials. However, the research publications on studying bolt materials are very limited, especially in a fire situation. There are only three or four publications existed in the literature. Although 20MnTiB as one of bolt materials has been examined in use for high-strength bolts [8], the elevated-temperature properties are extracted from metals before bolts are produced. It should be noted that the manufacturing process might have an influence on the material behavior. Therefore, it would be better to investigate the material behavior of high-strength bolts after production. Kodur et al. [9] was the first one looking at the deterioration of A325 and A490 bolt materials in a fire situation. Then Lange & Gonzalez [10] investigated the elevated-temperature material behavior of 10.9 carbon steel bolts. Although Ohlund et al. [11] attempted to discuss the physical properties of three types of carbon steel bolts in terms of their microstructural mechanisms, the extracted properties are very limited in application for fire safety analysis, even in connection design.

Although there are a cluster of metal materials available for bolt production (see Table 1), they generally fall into three sub- categories: medium carbon steel, carbon or alloyed steel with addition of boron, and alloyed steel. Medium carbon steel has a carbon content between 0.25 and 0.60% and its heat treatment can be performed easily. Therefore, grade 8.8 high-strength bolts are generally made out of this type of steel. For example, 45# steel is commonly used in China (equivalent to C45 in Germany). Boron is cost-effective as an alloying element for enhancement of hardenability in carbon or low-alloyed steels. The carbon boron steels are generally utilized for production of grade 8.8 and 10.9 high-strength bolts, for example, 10B21, 150M36 and 20MnTiB in Table 1. In addition, the alloyed steel shall contain at least one of the following elements with the minimum quantity specified: nickle 0.30%, chromium 0.30%, vanadium 0.10%, and molybdenum 0.20% from [6]. Addition of these alloyed elements is favorable to improvement of strength and ductility of these alloys after heat treatment. For example, the alloy steels 32CrB4 and 34Cr4 are commonly served as bolt materials in Europe [12,13], whereas 40Cr and ML40Cr are prevalent for production of 10.9 and 12.9 high-strength bolts in China, respectively [14,15]. It should be noted that ML40Cr is a cold-worked alloy with a tighter control of carbon compared with 40Cr alloy steel.

In the present study, an experimental scheme has been developed for investigation of physical properties of three sets of high-strength bolts: property classes 8.8, 10.9 and 12.9. These structural bolts are ordered to a Chinese standard GB/T 5782 [16]. The objective of this program is to deliver sufficient experimental data on the elevated-temperature properties of carbon steel bolts for fire safety analysis. Comparison has been performed for high-strength bolts which are produced from different bolt materials (see Table 1). This is to find out the influence of different bolt materials on reduction of physical properties at elevated temperatures. Eventually, the reduction models of physical properties have been proposed for carbon steel bolts in application for fire safety analysis.

Experimental program

Preparation of standard coupons

This experimental program covered three different sets of carbon steel bolts with property classes 8.8, 10.9 and 12.9. The ordered high-strength bolts were partially threaded with dimensional details as demonstrated in Fig. 1a. They complied with the published specifications GB/T 5782 and GB/T 3098.1 [16,17], where the provisions are almost in consistency with those in ISO 4014 [18] and ISO 898-1 [6]. Meanwhile, this study planned two hundred and seventy tensile tests at elevated temperatures. Each property class had ninety tensile tests with three duplicate coupons prepared for each test condition. The coupon specimens were milled from the previously ordered high-strength bolts with geometrical details complying to BS EN ISO 6892-2 (see Fig. 1b) [19]. The lower and upper ends of each coupon were threaded for the gripping jaws (see Fig. 2a). The lower end was free to move before starting tensile tests.

Heating and cooling

The elevated-temperature tests were performed under tension. The heat was provided by an electronically controlled furnace with the maximum heating temperature of 1000 °C (see Fig. 2). During the heating phase, three thermocouples (K-type) were mounted into the furnace for controlling and monitoring the furnace temperatures. These thermocouples were placed as near to the specimen as possible. The coupon specimens were heated up to nine different target temperatures (100, 200, 300, 400, 500, 600 700, 800 and 900 °C) at a constant heating rate of 5–10 °C/min [4], followed by a soaking period of 20 min before loading. During heating, the coupon temperature shall not exceed the specified temperature with its tolerances in Section 9.3 of reference [19]. The characteristic temperature–time curve was demonstrated in Fig. 2b, and air cooling was employed for cooling samples to room temperature.

Testing

The coupon tests was performed in tension with a servo-controlled loading system (Instron 8862). Three duplicate speci- mens were prepared for each test condition. The strains were recorded by a high-temperature extensometer with its gauge length of 12.5 mm (see Fig. 2a). The majority of coupon tests (261 coupons) were completed complying with BS EN ISO 6892-2 [19]. It should be noted that material properties determined within tensile tests at elevated temperatures should be determined at a slower strain (stressing) rate than at room

Table 1
Materials and chemical compositions.

Grade	Steel name	Specification	Source	Process	Quenching T /°C	Tempering T /°C	C	Si	Mn	P
8.8	45#	GB/T 699	Present study /C	N/A	840	600	0.44	0.22	0.55	0.016
	Type 9	BS 3111–1	Kirby (1995) /C	Cold forged	850	450–500	0.21	0.25	1.02	0.009
	150 M36	BS 970–1	Kirby (1995) /C	Hot forged	900	600–620	0.41	0.16	1.61	0.021
	SAE 10B38	SAE J403	Kodur et al. (2017) /C	Cold forged	870	530	0.399	0.27	0.736	0.0117
	SAE 10B21	SAE J403	Kodur et al.(2017) /C	Cold forged	870	475	0.223	0.253	0.851	0.0132
10.9	40Cr	GB/T 3077	Present study /C	N/A	850	520	0.4	0.26	0.62	0.016
	20MnTiB	GB/T 3077	Li et al. (2003) /S	N/A	860	200	0.17–0.24	0.17–0.37	1.3–1.6	≤0.035
	32CrB4	EN 10263–4	Lange et al. (2012) /S	Cold forged	860	N/A	0.30–0.34	≤0.30	0.60–0.90	0.025
	33B2	EN 10263–4	Ohlund et al. (2016) /C	Cold forged	890	460	0.32	0.09	0.72	0.01
	SCM435	JIS G 4053	Yahyai et al. (2018) /C	Hot forged	870	620	0.357	0.215	0.729	0.0133
	SAE 10B21	SAE J403	Yahyai et al. (2018) /C	Cold forged	870	475	0.223	0.253	0.851	0.0132
12.9	ML40Cr	GB/T 6478	Present study /S	N/A	820–860	540–680	0.38–0.45	≤0.30	0.60–0.90	≤0.035
	34Cr4	EN 10083–3	Ohlund et al. (2016) /C	Cold forged	890	460	0.36	0.1	0.85	0.006

Grade	S	Cr	Mo	Ni	Al	B	Cu	Nb	Ti	V
8.8	0.012	0.3	/	0.2	/	/	0.1	/	/	/
	0.009	0.23	0.021	0.1	0.029	0.0024	0.14	< 0.005	0.042	< 0.005
	0.038	0.13	0.13	0.12	0.018	< 0.0005	0.23	< 0.005	< 0.005	< 0.005
	0.0047	0.0733	0.005	0.0085	0.0267	0.0015	0.0779	0.0023	0.0365	< 0.002
	0.007	0.1415	0.005	0.0171	0.0184	0.001	0.0893	0.002	0.0354	< 0.002
10.9	0.005	0.94	/	/	/	/	/	/	/	/
	≤0.035	/	/	/	/	0.0005–0.00-35	/	/	0.04–0.10	/
	0.025	0.90–1.20	/	/	/	0.0008–0.005	0.25	/	/	/
	0.01	0.23	0.008	0.04	0.031	0.002	/	/	0.051	0.004
	0.0077	1.06	0.212	≤0.005	0.0263	< 0.001	0.0172	< 0.002	< 0.002	< 0.002
	0.007	0.1415	0.005	0.0171	0.0184	0.001	0.0893	0.002	0.0354	< 0.002
12.9	≤0.035	0.90–1.20	/	/	/	/	/	/	/	/
	0.007	1.09	0.05	0.05	0.036	/	/	/	0.001	0.003

/C means chemical compositions from material certificates; /S means chemical compositions from standards.

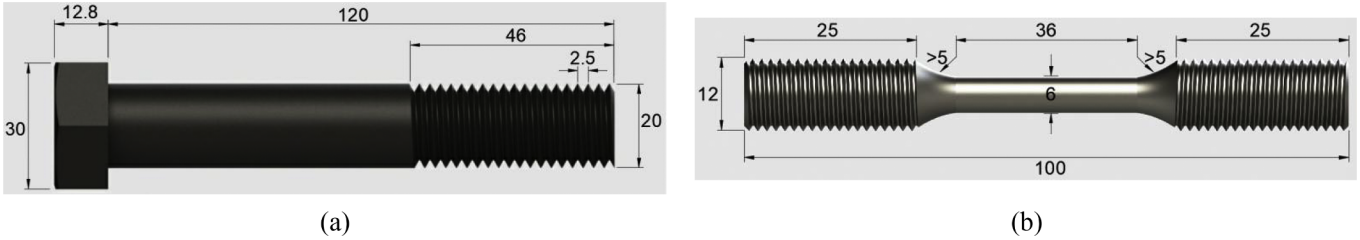

Fig. 1. Carbon steel bolts (a) Partially threaded; (b) Coupon specimen (unit: mm).

temperature [19]. Therefore, two estimated strain rates ($\dot{\varepsilon}_{Lc}$) of 0.005/min and 0.03/min were employed for determination of 0.2% proof strength and ultimate tensile strength, respectively. In contrast, nine coupons were tested at room temperature complying to BS EN ISO 6892-1 [20]. Strain rates employed are slightly faster than those utilized at elevated temperatures. The rate ($\dot{\varepsilon}_{Lc}$) of 0.01/min was used for determination of 0.2% proof strength, whereas 0.05/min was for ultimate tensile strength. In order to achieve the specified strain rates, the stroke rate (crosshead separation rate) was set up as the product (v_c) of parallel length of coupon specimen (L_c) and estimated strain rate ($\dot{\varepsilon}_{Lc}$). After tensile tests completed, the full range stress–strain curves were produced for the required material properties.

Experimental results and discussion

Stress–strain curves

The elevated-temperature stress–strain curves are demonstrated for carbon steel bolts (see Fig. 4). It should be noted that the stress–strain curves exhibited a linear elastic behavior before material yielding, whereas a nonlinear material behavior was observed after the yielding. Since yield plateau was not well-defined for these high-strength materials, 0.2% proof strength was determined as the yielding strength (f_{yT}). There are five key elevated-temperature material properties extracted from the recorded stress–strain curves, containing Young's modulus (E_{sT}), 0.2% proof strength (f_{yT}), ultimate strength (f_{uT}), ultimate strain (ε_{uT}) and fracture strain (ε_{fT}) as shown in Table 2 and Fig. 3. The subscript T indicated the material properties extracted from the elevated-temperature tests, whereas E_s, f_y, f_u, ε_u, and ε_f may be used for indicating the properties at room temperature.

In addition, Fig. 5 demonstrated the failure modes of coupons and

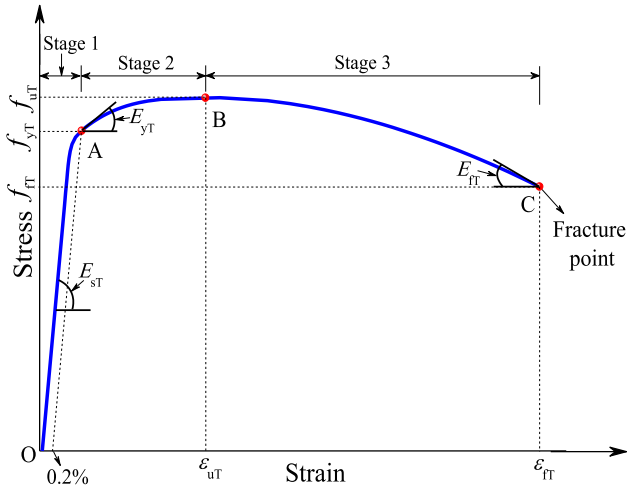

Fig. 3. Key parameters to define a full-range stress–strain curve (modified from Tao et al. [21]).

their failure surfaces. It should noted that under 400 °C the neck-shrink phenomenon and shear lips both were observed in almost all tested coupons, while above this temperature only the neck-shink failure was observed from the tested samples. This indicated a ductile failure mechanism resulting from excessive large deformation at higher temperatures.

Young's modulus

The elastic modulus is defined as the initial slope of a stress–strain

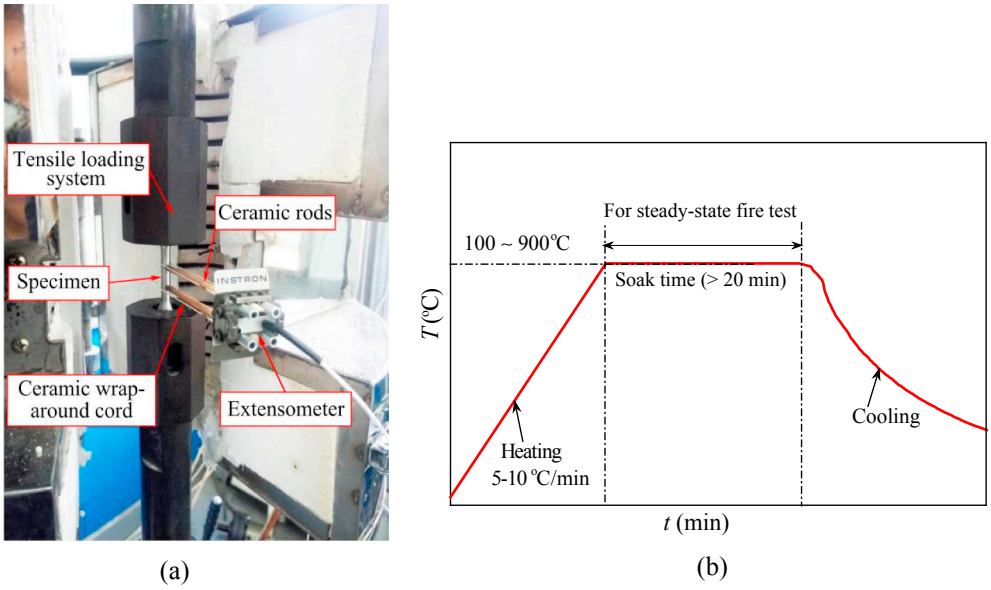

Fig. 2. Experimental setup: (a) Tensile loading system with installed coupon; (b) Temperature-time curve.

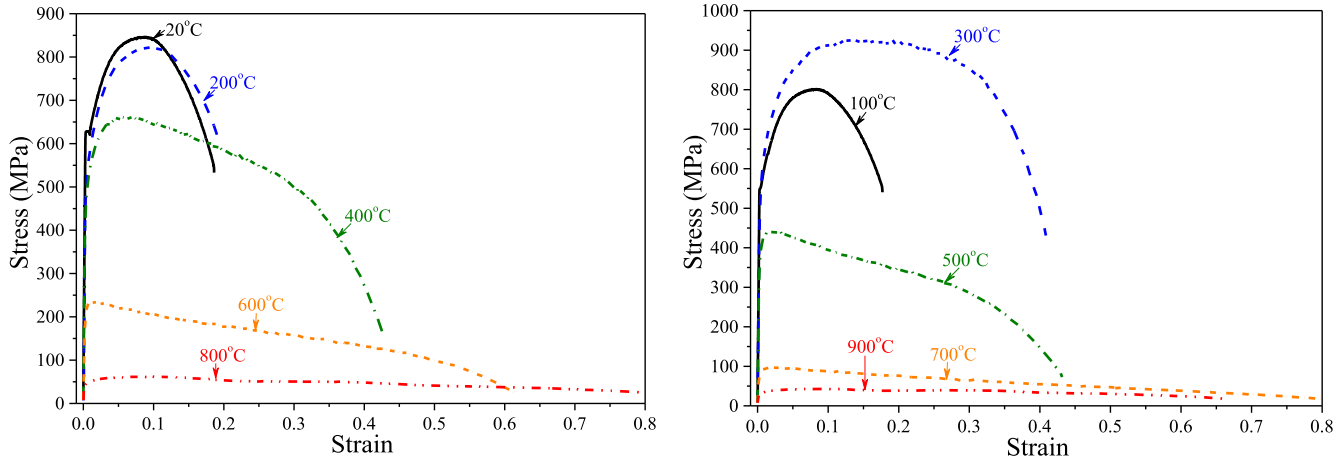

(a)

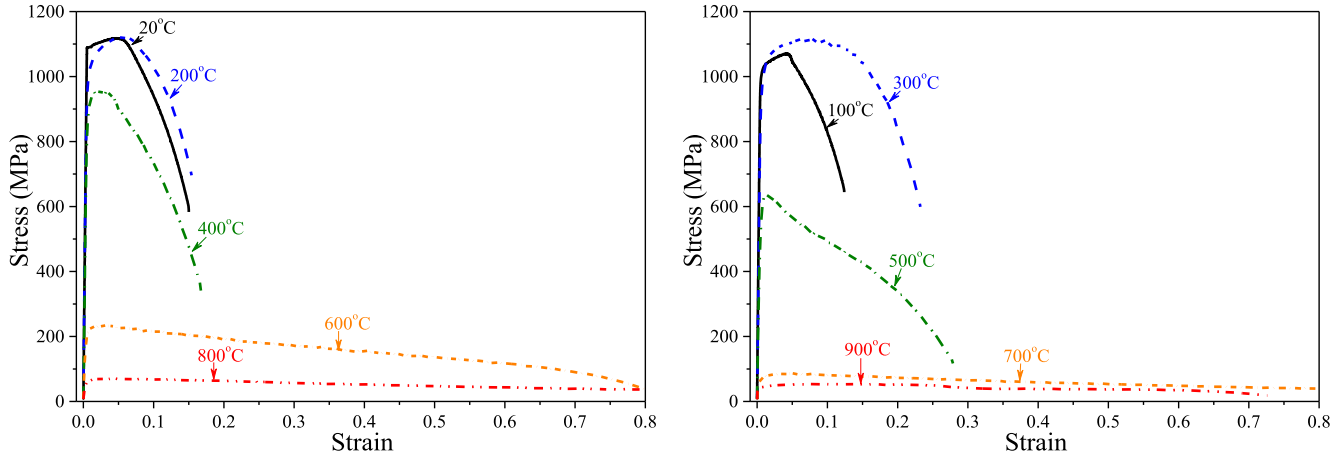

(b)

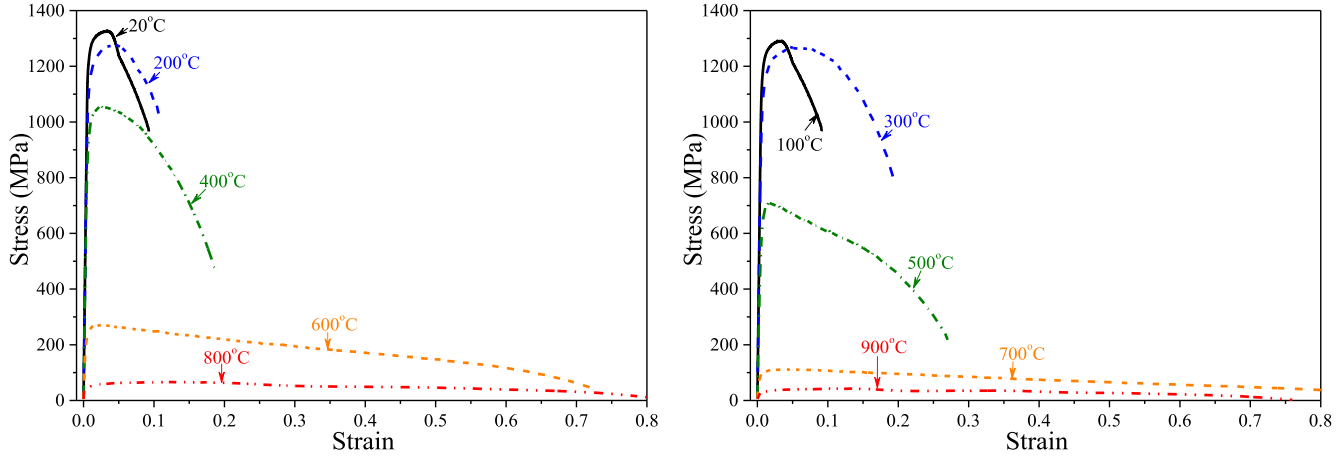

(c)

Fig. 4. Stress–strain curves of carbon steel bolts (a) Grade 8.8; (b) Grade 10.9; (c) Grade 12.9.

curve for each coupon. The E_{sT}/E_s ratio represents the changes of this material property caused by temperature (T). Fig. 5a demonstrated the deterioration of Young's modulus as the ratio of E_{sT}/E_s for high-strength bolts compared with those from Li et al. [8] and Lange & Gonzalez [10]. In general, this property experienced a slight reduction below 400 °C, then followed by a dramatic drop-off from 400 to 700 °C, and finally approaching a small value less than 0.1 until 900 °C. This finding has been confirmed in references [8,10] in the same plot. However, it

Table 2
Material properties of high-strength structural bolts.

	E_{sT}						f_{yT}			
	8.8		10.9		12.9		8.8		10.9	
	Mean (GPa)	COV	Mean (GPa)	COV	Mean (GPa)	COV	Mean (MPa)	COV	Mean (MPa)	COV
20	211.7	0.025	214.5	0.031	211.1	0.002	668.2	0.144	1085	0.015
100	205.1	0.012	224.6	0.071	214.4	0.018	577.5	0.054	1018	0.019
200	204.8	0.076	216.1	0.034	207.1	0.036	543.8	0.125	969.0	0.011
300	203.6	0.045	206.5	0.013	204.1	0.019	575.0	0.099	946.3	0.035
400	197.0	0.041	186.6	0.046	181.4	0.014	493.7	0.122	858.5	0.036
500	169.4	0.057	144.9	0.131	134.7	0.039	374.8	0.112	572.3	0.188
600	89.90	0.057	72.81	0.059	95.69	0.073	213.4	0.012	214.9	0.146
700	48.65	0.123	33.06	0.045	53.50	0.023	84.89	0.031	63.51	0.035
800	38.61	0.002	24.84	0.141	36.32	0.072	47.43	0.101	54.56	0.046
900	17.64	0.072	15.78	0.210	16.74	0.038	24.66	0.135	34.26	0.255

	f_{yT}		f_{uT}						ε_{uT}	
	12.9		8.8		10.9		12.9		8.8	
	Mean (MPa)	COV	Mean (MPa)	COV	Mean (MPa)	COV	Mean (MPa)	COV	Mean (%)	COV
20	1210	0.023	865.3	0.076	1114	0.018	1310	0.020	8.235	0.134
100	1175	0.004	813.6	0.037	1075	0.019	1287	0.004	7.914	0.112
200	1107	0.007	835.7	0.061	1118	0.015	1288	0.005	8.483	0.152
300	1055	0.015	939.5	0.043	1111	0.026	1269	0.014	14.96	0.050
400	933.7	0.024	676.2	0.068	941.5	0.037	1058	0.019	6.090	0.111
500	604.6	0.024	436.2	0.081	641.5	0.170	701.4	0.034	2.324	0.264
600	224.1	0.017	236.1	0.009	258.2	0.164	270.9	0.010	1.464	0.070
700	85.43	0.020	98.76	0.025	85.42	0.026	113.8	0.007	2.696	0.285
800	42.53	0.021	63.72	0.028	71.15	0.019	67.13	0.008	8.022	0.173
900	23.86	0.033	41.98	0.027	50.04	0.115	42.93	0.019	10.98	0.202

	f_{yT}	ε_{uT}				ε_{fT}			
	10.9	10.9		12.9		8.8		10.9	12.9
	Mean (MPa)	Mean (%)	COV	Mean (%)	COV	Mean (%)	COV	Mean (%)	COV
20	1085	4.455	0.068	3.250	0.060	18.79	0.106	14.72	0.065
100	1018	4.378	0.078	3.181	0.092	17.65	0.071	13.14	0.056
200	969.0	5.192	0.119	4.245	0.068	17.63	0.080	15.36	0.031
300	946.3	7.820	0.152	5.787	0.173	37.24	0.121	24.91	0.066
400	858.5	2.183	0.077	2.625	0.093	39.84	0.126	18.29	0.012
500	572.3	1.360	0.102	1.796	0.054	37.13	0.317	30.27	0.092
600	214.9	2.367	0.345	2.999	0.113	59.43	0.112	77.65	0.022
700	63.51	4.742	0.093	3.962	0.085	74.38	0.071	142.0	0.045
800	54.56	6.697	0.653	13.76	0.119	73.07	0.140	115.8	0.058
900	34.26	11.21	0.022	12.53	0.032	65.23	0.019	68.31	0.079

should be noted that the experimental data are very limited at the temperatures above 700 °C. As seen in Fig. 5a, reference [7] has no data above 700 °C, whereas Lange & Gonzalez [9] only gives a ratio of 0.027 as the reduction factor of Young's modulus at 800 °C. This is much less than the ratio of 0.12 from the present study. This finding could be explain as different bolt materials were employed for fastener production, as displayed in Table 1, with accounting for the influence of different manufacturing processes.

It should noted that there is no standard for the Young's modulus reduction of carbon steel bolts at elevated temperatures. Therefore, reduction factors of carbon steels from EC3 Part 1-2 [22] and AS 4100 [23] are employed, as plotted in Fig. 6b, compared with the ratios derived from coupon tests of the present study. It is worthy of noticing that the reduction factors from both standards cannot deliver a reliable prediction for the deterioration of carbon steel bolts. As can be seen from Fig. 6b, underestimation of the Young's modulus was observed for the reduction factors from EC3 Part 1-2 at the temperatures lower than 500 °C, whereas the standard AS 4100 produced an overestimation of the Young's modulus values from 600 to 900 °C. As a consequence of this, a specific reduction model of Young's modulus was proposed for carbon steel bolts at elevated temperatures. This has been expressed in Eq. (1), as displayed in Fig. 6.

$$\frac{E_{sT}}{E_s} = \begin{cases} 1-(T-20)/6000 & 20^\circ\,C \le T < 300^\circ C \\ 1-(T-275)/500 & 300^\circ\,C \le T < 700^\circ C \\ 1-(T+1580)/2700 & 700^\circ\,C \le T < 900^\circ C \end{cases} \quad (1)$$

0.2% proof strength

In literature, studying 0.2% proof strength (f_{yT}) of carbon steel bolts was very limited in a fire situation. This is caused by shortage of relevant experimental data. In order to fill this gap in knowledge, 0.2% proof strengths at elevated temperatures were extracted from the stress–strain curves of standard coupon tests. The ratio of f_{yT}/f_y indicated the deterioration of f_{yT} on the basis of f_y at room temperature. This ratio is a function of temperature T as the experimental values of f_{yT} collected in Table 2 correspond to their tested temperatures. As seen from Fig. 6a, there is a slight decrease observed in proof strength f_{yT} from 20 to 300 °C, followed by a dramatic fall-off between 400 and 700 °C, and eventually reaching the bottom at 900 °C. In addition, the f_{yT}/f_y ratio of 20MnTiB was derived from strength values of f_{yT} taken from [8], which has been plotted in Fig. 7a as well. It was found that these materials employed for high-strength bolts are much alike in their proof strength reductions at elevated temperatures.

In addition, a comparison was performed for the f_{yT}/f_y ratio between the tested values in this study and strength reduction factors of structural steels from standards (see Fig. 7b). This is because there is no standard used for yield strength reduction of carbon steel bolts. Although four specifications were employed in this comparison including AS 4100 [23], GB 51249 [24], EC3 Part 1-2 [22], and AISC 360-10 [25], reduction factors from two standards (EC3 Part 1-2 and AISC 360-10) are almost the same in their values. Therefore, only three reduction models are shown in Fig. 6b. In addition, it should be noted that if using

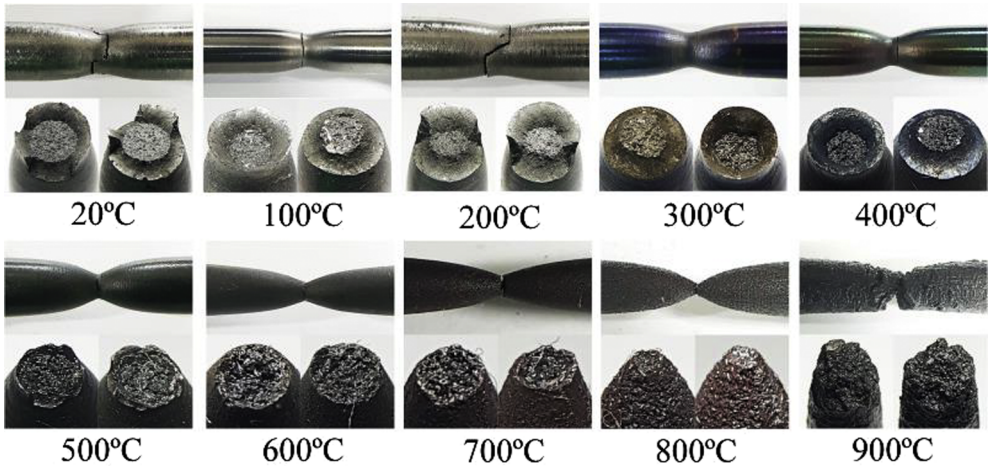

Fig. 5. Failed specimens for carbon steel bolts.

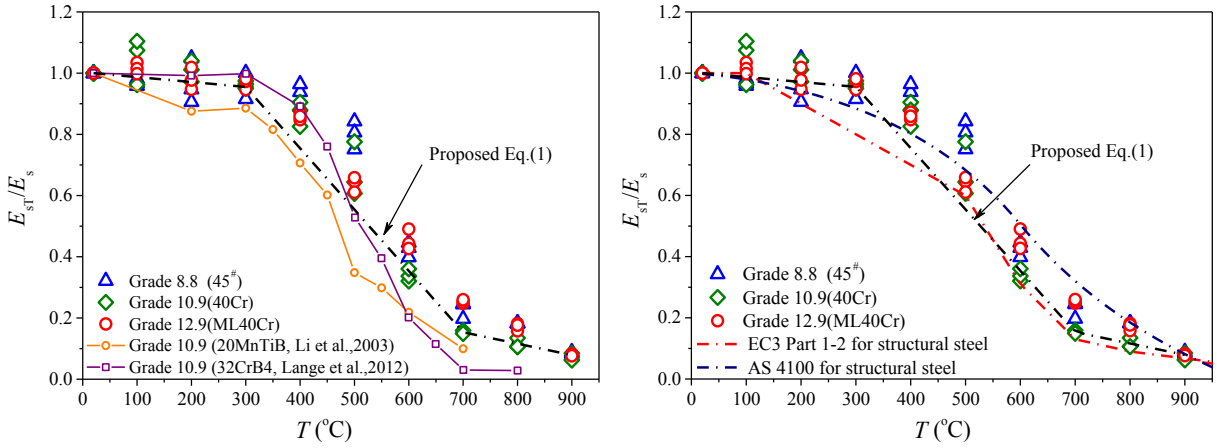

Fig. 6. Deterioration of Young's modulus: (a) Comparison with other tested results; (b) Comparison with standards.

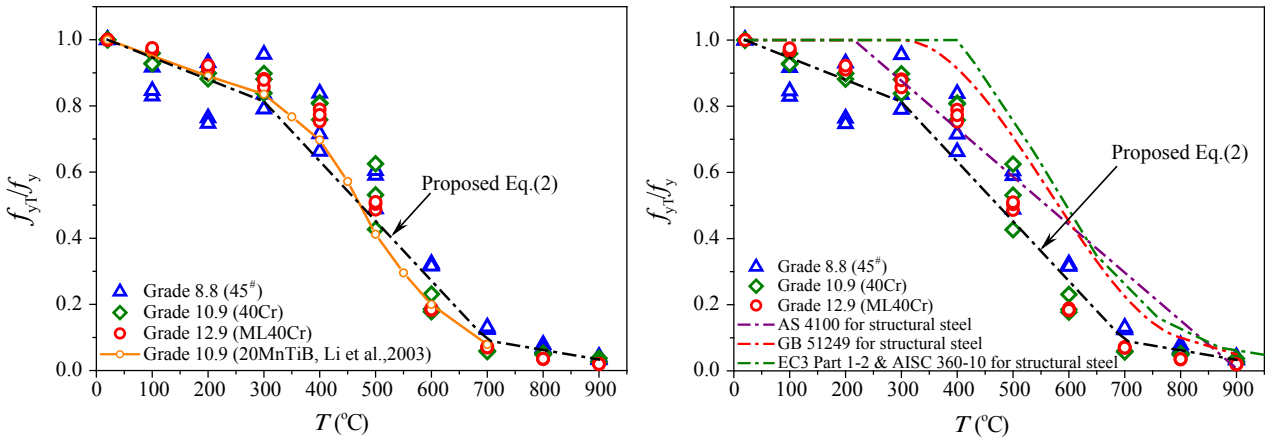

Fig. 7. Deterioration of 0.2% proof strength f_{yT}: (a) Comparison with other tested results; (b) Comparison with standards.

these factors for estimating the yield strength reduction at elevated temperatures, they generally overestimated the yield strength of carbon steel bolts. Therefore, a simplified reduction model was proposed for the yield strength of carbon steels bolts used at elevated temperatures (see Eq. (2) in Fig. 7b).

$$\frac{f_{yT}}{f_y} = \begin{cases} 1.0 - (T - 20)/1500 & 20^\circ\,C \le T < 300^\circ C \\ 1.0 - (T - 200)/540 & 300^\circ\,C \le T \le 700^\circ C \\ 1.0 - (T + 3080)/4080 & 700^\circ\,C \le T \le 900^\circ C \end{cases} \quad (2)$$

Ultimate tensile strength (UTS)

The ultimate tensile strength f_{uT} was determined as the maximum stress in a stress–strain curve. The ratios of f_{uT}/f_u are derived from the material strengths of coupon tests compared with other published results as displayed in Fig. 8 [4,8–10]. This ratio is a function of temperature *T,* which indicated the deterioration of f_{uT} for carbon steel bolts. It should noted that in different bolt materials have an analogical strength reduction at elevated temperatures. From this figure, an up-and-down fluctuation in f_{uT}/f_u was observed between room temperature and 300 °C, then followed by a remarkable reduction in strength up to 900 °C. Meanwhile, the existing reduction models (of f_{uT}/f_u) from Kirby [4], EC3 Part 1-2 [22] and BS 5950-8 [26] are compared with the present test results displayed in Fig. 8b. It should be noted that these models are generally capable of capture the downward trend of the tensile strength. The reduction models from EC3 and BS 5950 are almost the same for carbon steels bolts, which demonstrated a conservative prediction in f_{uT} at temperatures lower than 400 °C and a reasonable prediction hereafter. In contrast, the Kirby's model has a better prediction at temperatures below 400 °C, but with a slightly unsafe estimation of bolt strength at higher temperatures. For fire safety consideration, the reduction factors proposed from EC3 Part 1-2 are therefore accepted for the tensile strength prediction at elevated temperatures.

Ultimate strain and fracture strain

ε_{uT} is the strain corresponding to UTS, generally including the uniform deformation before coupon necking. The ratio of $\varepsilon_{uT}/\varepsilon_u$ demonstrated the change of the ultimate strain of elevated-temperature (ε_{uT}) to the strain (ε_u) at room temperature (see Fig. 9). It should be noted that ε_{uT} increased slightly until 300 °C possibly due to uniform thermal expansion during testing, whereas there is a noticed decrease observed in this strain up to approximately 600 °C, then increased again until 900 °C. The cause of this fluctuation in ε_{uT} is still not clear in terms of change of crystalline structure. However, there are two important facts involved in contribution to this change: a) material recrystallization involved with formation of a new grain structure starting from 450 °C; b) phase transformation of metal materials with material crystal structure transformed to austenite at 725 °C. In other words, ε_{uT} is seriously influenced by formation of new grains and rearrangement of atoms. However, it should also be noted that the changes of ultimate strain for three sets of high-strength bolts are not exactly the same as demonstrated in Fig. 9. This is possibly due to different bolt materials essentially applied for production with a slightly different manufacturing process, for example, different quenching and tempering temperatures [4]. In addition, for demonstrating the changes of ε_{uT} at elevated temperatures, a set of analytical equations was proposed for

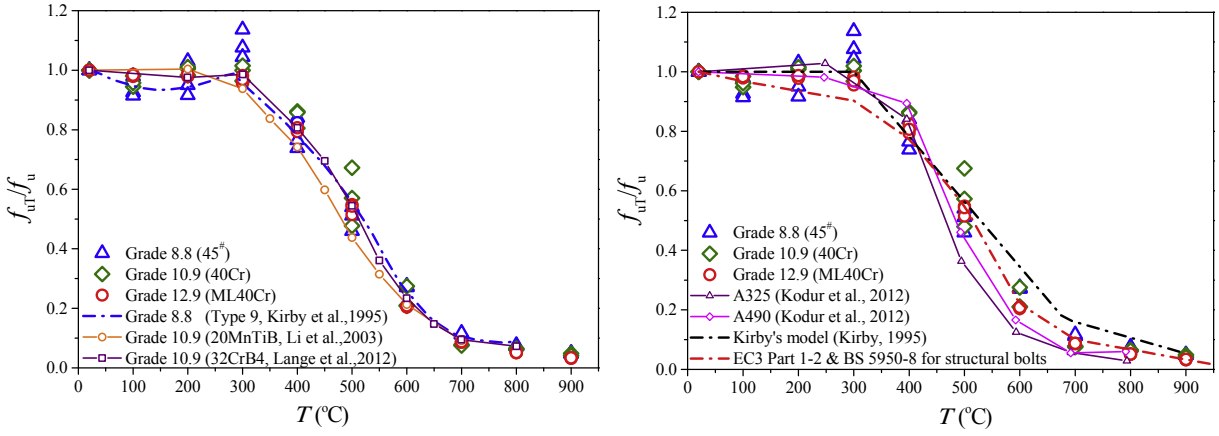

Fig. 8. Deterioration of tensile strength f_{uT}: (a) Comparison with other tested results; (b) Comparison with standards.

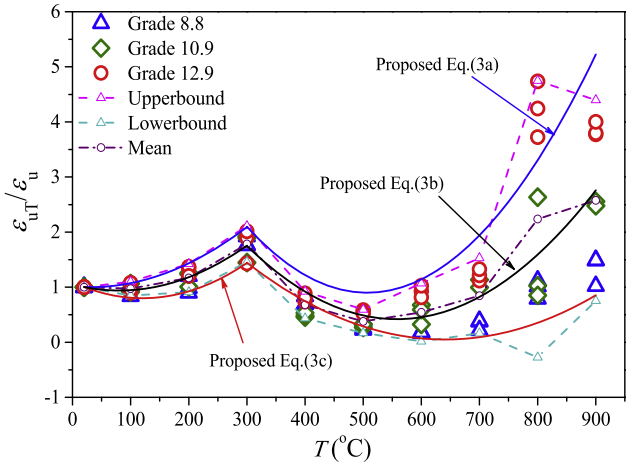

Fig. 9. Ultimate strain (ε_{uT}).

high-strength bolts as displayed in Eq. (3).

ε_f is the engineering strain at fracture served as a function of the geometry of coupon specimen and its material. It covers the deformation in the necked region and unnecked region together. As a consequence of this, this strain is only a crude measure of material ductility. Likewise, ε_{fT} is the fracture strain at elevated temperatures. We can simply assume that ε_{fT} is dependent on ε_{uT} in a fire situation because of material consistency in one coupon. Therefore, the ratio of $\varepsilon_{fT}/\varepsilon_{uT}$ indicated the changes of ε_{fT} with respect to the corresponding ε_{uT} at elevated temperatures as illustrated in Fig. 10. It should be noted that ε_{fT} is proportional to ε_{uT} as the ratio of these two strains is a constant until 300 °C. However, in the temperature range of 400 to 600 °C this ratio has a drastic rise. This was caused by reduction of uniform deformation (shown in Fig. 9) and remarkable increase of necking deformation. In contrast, after 600 °C this ratio was decreased drastically. This might be caused by an increase of uniform deformation. After complete transformation to austenite at 900 °C, this ratio becomes a constant again shown in Fig. 10. As a consequence of this analysis, another set of analytical equations was proposed for determining the boundaries of variation of ε_{fT} for three sets of high-strength bolts as displayed in Eq. (4).

$$\frac{\varepsilon_{uT}}{\varepsilon_u}=\begin{cases}0.20\times\left(\frac{T}{100}-1.2\right)^2+0.81 & 20\le T\le 300°C \quad \text{Lower bound}\\ 0.145\times\left(\frac{T}{100}-6.4\right)^2-0.21 & 300<T\le 900°C \quad \text{(Grade 8.8)}\end{cases} \tag{3c}$$

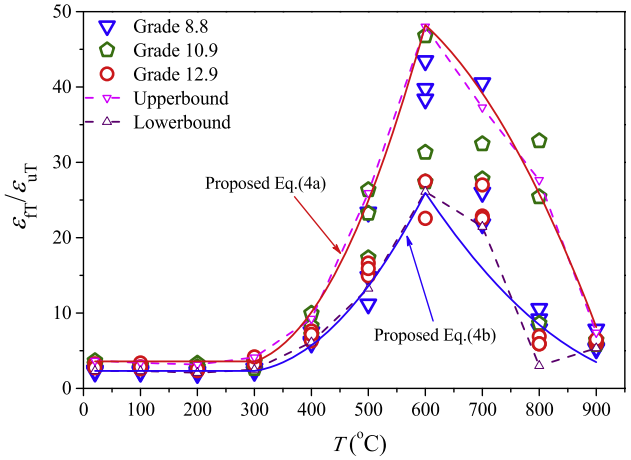

Fig. 10. Fracture strain (ε_{fT}).

$$\frac{\varepsilon_{uT}}{\varepsilon_u}=\begin{cases}0.172\times\left(\frac{T}{100}-0.8\right)^2+0.94 & 20\le T\le 300°C \quad \text{Mean}\\ 0.20\times\left(\frac{T}{100}-5.6\right)^2+0.46 & 300<T\le 900°C \quad \text{(Grade 10.9)}\end{cases} \tag{3b}$$

$$\frac{\varepsilon_{uT}}{\varepsilon_u}=\begin{cases}0.15\times\left(\frac{T}{100}-0.3\right)^2+1.0 & 20\le T\le 300°C \quad \text{Upper bound}\\ 0.28\times\left(\frac{T}{100}-5.1\right)^2+0.85 & 300<T\le 900°C \quad \text{(Grade 12.9)}\end{cases} \tag{3a}$$

$$\frac{\varepsilon_{fT}}{\varepsilon_{uT}}=\begin{cases}3.58 & 20\le T\le 300°C\\ 4.1\times\left(\frac{T}{100}-2.7\right)^2+3.42 & 300<T\le 600°C \quad \text{Upper bound}\\ -2\times\left(\frac{T}{100}-4.2\right)^2+54.4 & 600<T\le 900°C\end{cases} \tag{4a}$$

$$\frac{\varepsilon_{fT}}{\varepsilon_{uT}}=\begin{cases}2.31 & 20\le T\le 300°C\\ 2.2\times\left(\frac{T}{100}-2.7\right)^2+2.3 & 300<T\le 600°C \quad \text{Lower bound}\\ -0.0705\times(T-600)+26.54 & 600<T\le 900°C\end{cases} \tag{4b}$$

Discussion

The preceding discussion revealed the deterioration of material properties of high-strength bolts at elevated temperatures, compared with different bolt materials coming from different countries. It should be noted that strength reductions of carbon steel bolts in a fire are almost the same in spite of different materials employed for bolt production. Hereafter, the elevated- temperature material properties of high-strength bolts are compared with high-strength structural steels (reported in previous studies [27–32]). The proposed reduction models of carbon steel bolts were applied in the following plots as a representation of their characteristic material properties. However, high-strength steels with yield strengths higher than 1080 MPa or lower than 640 MPa are not included in this study, as these steels are not comparable to the bolts in terms of yield strength.

Fig. 11a demonstrated the Young's modulus reduction coefficients of high-strength bolts at elevated temperatures compared with high-strength steels. The solid points in this figure represented the calculated reduction factors from coupon tests of high-strength bolts, whereas hollow dots indicated the test results extracted from high-strength steels. It can be found that about 5–18% reduction of Young's modulus was observed for high-strength bolts and steels under 400 °C, while the Young's modulus reduction of high-strength bolts are generally faster than most of high-strength steels at the temperatures after 300 °C. This deviation might be caused by different chemical compositions, microstructures and manufacture processes between high-strength steels and carbon steel bolts [27].

In addition, the reduction factors of f_y and f_u to high-strength bolts are displayed in Fig. 11b and c, respectively. These factors are compared with those of high-strength steels shown in the same plots. It should be noted that there are some deviations observed in the strength reduction of f_y and f_u. Obviously, about 20% strength reduction (f_y) is observed for high- strength bolts and some of high-strength steels below 400 °C, whereas there is no significant deterioration observed for f_u in the same temperature range. We may attribute the reduction of f_y to the temperature-induced change of material nonlinearity. In contrast, the stabilized f_u may be due to no significant changes in crystalline structures before 400 °C. For temperatures after 300 °C, strength reductions in f_y and f_u are very similar, which are obviously lower than the majority of high-strength steels. The deviation in material strength may be attributed to the different manufacturing processes employed for production and relatively higher carbon content in high-strength bolts

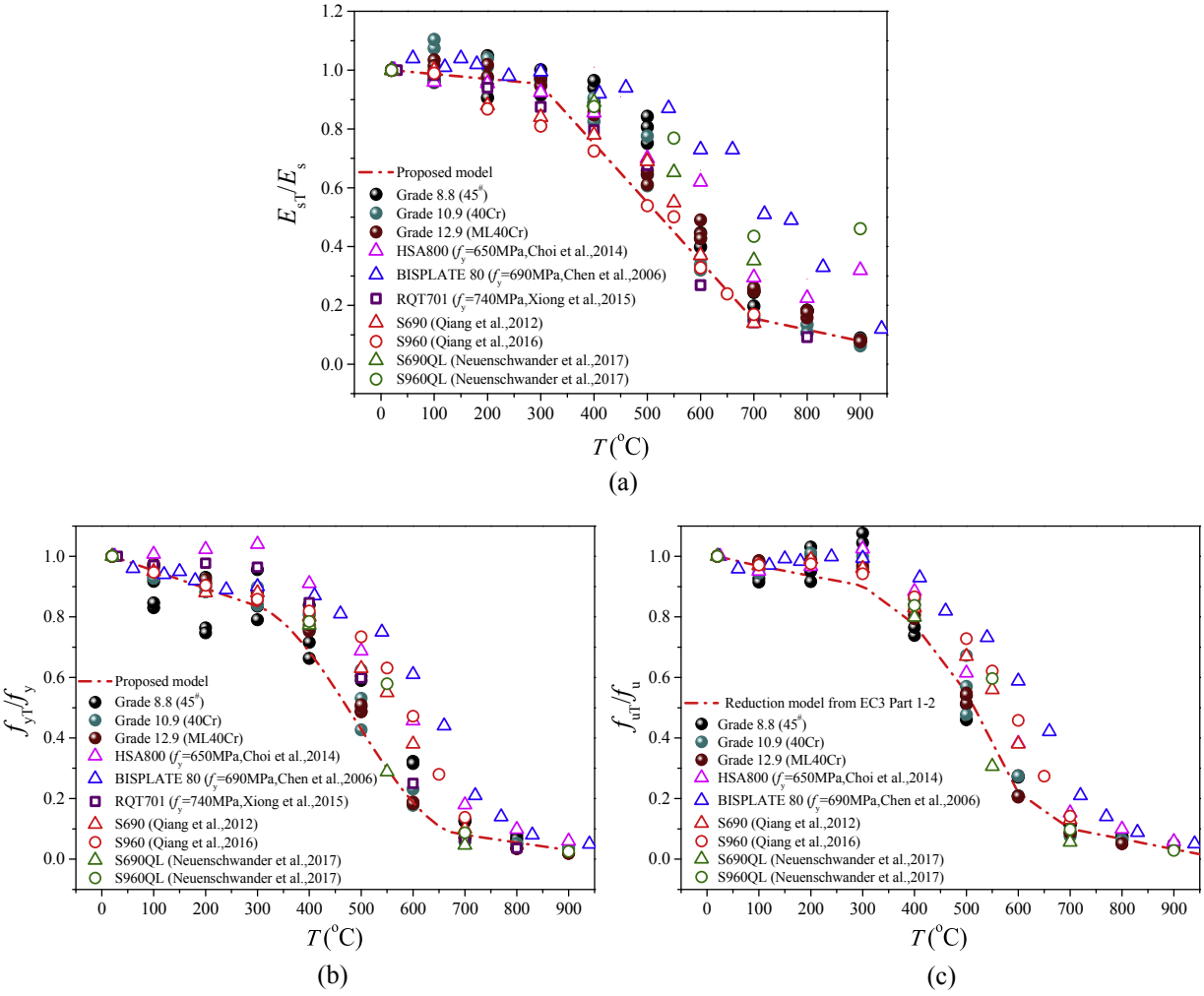

Fig. 11. Comparison between carbon steel bolts and high-strength steels: (a) E_{sT}/E_s (b) f_{yT}/f_y (c) f_{uT}/f_u.

compared with high-strength steels as displayed in Table 2.

Conclusion

This experimental study performed a large series of elevated-temperature coupon tests on high-strength bolts employed for investigation of their material behavior at elevated temperatures. The extracted material properties from the preceding tests are compared with the physical properties of carbon steel bolts and high-strength steels in the published journals. A couple of conclusions may be drawn within the scope of this research:

a) Although different materials are employed for production of high-strength bolts in the world, the material proprieties produced at elevated temperatures are very much alike in their reductions. It should be noted that the reduction model from EC3 Part 1-2 can be employed for tensile strength reduction at elevated temperatures, whereas the reduction factors of yield strength and Young's modulus have to be proposed for high-strength bolts.
b) With respect to the strain, it should be noted that changes in crystalline structures (material recrystallization and phase transformation) has a significant influence on material strains (ε_{uT} and ε_{fT}). This was displayed as various peaks and troughs in ε_{uT} and ε_{fT} in the temperature range of 400–900 °C (see Figs. 9 and 10), whereas under 400 °C ε_{uT} and ε_{fT} demonstrated a consistency in uniformly increasing the deformation.
c) A comparison has been performed for carbon steels bolts and high-strength steels. It should be noted that a similar trend in reduction of material properties was found for carbon steel bolts and high-strength steels before 400 °C, while after this temperature the material deterioration of carbon steel bolts was generally faster than most of high-strength steels.

Acknowledgements

The authors would like to acknowledge the financial support from National Natural Science Foundation of China (NSFC Project No. 51578092), 111 Project of China (Grant No. B18062), Chongqing Science and Technology for Fundamental Science and Cutting-edge Technology (CSTC Project No. cstc2016jcyjA1097) and Chongqing Science and Technology Commission for Technology Innovation of Social Business and Insurance (CSTC Project No. cstc2015shmszx1227). The research is also partly supported by Project of Science and Technology of Shandong Colleges and Universities (Project No: J14LG52), and Research Supporting Project of Shandong Polytechnic (Project No: KY-W201403). Comments and assistance toward this research project from Mr. JL Wen and Mr. G Yao at Shenyang National Laboratory for Material Science of the Chinese Academy of Sciences, are also highly appreciated. My student Mr. Xin Lei should be also acknowledged for his faithful support.

Appendix A. Supplementary data

Supplementary data to this article can be found online at https://

doi.org/10.1016/j.rinp.2019.102156.

References

[1] Wang YC, Davison JB, Burgess IW, Plank RJ, Yu HX, Dai XH, et al. The safety of common steel beam/column connections in fire. Struct Engineer 2010;88:26–35.
[2] Lamont S. The behavior of multi-storey composite steel framed structures in response to compartment fires [PhD Thesis]. Edinburgh: The University of Edinburgh; 2001.
[3] Hu Y, Shen L, Nie S, Yang B, Sha W. FE simulation and experimental tests of high-strength structural bolts under tension. J Constr Steel Res 2016;126:174–86.
[4] Kirby BR. The behaviour of high-strength grade 8.8 bolts in fire. J Constr Steel Res 1995;33:3–38.
[5] Grimsmo EL, Aalberg A, Langseth M, Clausen AH. Failure modes of bolt and nut assemblies under tensile loading. J Constr Steel Res 2016;126:15–25.
[6] ISO. ISO 898–1 Mechanical properties of fasteners made of carbon steel and alloy steel. Switzerland: International Organization for Standardization; 2009.
[7] Hu Y, Davison JB, Burgess IW, Plank RJ. Fire performance of grade 8.8 bolts. Eurosteel 2011: 6th European Conference on Steel and Composite Structures, Budapest, Hungary, 2011.08.31–2011.09.02. 2011. p. 231–7.
[8] Li G, Li M, Jiang S, Yin Y, Chen K. Experimental studies on the properties of constructional steel at elevated temperatures. J Struct Eng 2003;129:1717–21.
[9] Kodur V, Kand S, Khaliq W. Effect of temperature on thermal and mechanical properties of steel bolts. J Mater Civil Eng 2012;67:765–74.
[10] Gonzalez F, Lange J. Behavior of high-strength grade 10.9 bolts under fire conditions. Struct Eng Int 2012;22:470–5.
[11] Ohlund CEIC, Lukovic M, Weidow J, Thuvander M, Offerman SE. A Comparison between ultra-high-strength and conventional high-strength fastener steels: mechanical properties at elevated temperature and microstructural mechanisms. ISIJ Int 2016;56:1874–83.
[12] CEN. BS EN 10083-3, steels for quenching and tempering – part 3: technical delivery conditions for alloy steels. Brussels: European Committee for Standardization; 2006.
[13] CEN. BS EN 10263-4, steel rod, bars and wire for cold heading and cold extrusion – part 4: technical delivery conditions for steels for quenching and tempering. Brussels: European Committee of Standardization; 2005.
[14] SAC. GB/T 3077, Alloy structure steel. Standardization Administration of the People's Republic of China, Beijing, 2015.
[15] SAC. GB, T 6478, Steels for cold heading and cold extruding. Standardization Administration of the People's Republic of 2001 China, Beijing.
[16] SAC. GB, T 5782, Hexagon head bolts. Standardization Administration of the People's Republic of 2016 China, Beijing.
[17] SAC. GB, T 3098.1, Mechanical properties of fasteners - Bolts, screws and studs. Standardization Administration of the People's Republic of 2010 China, Beijing.
[18] ISO. ISO 4014, Hexagon Head Bolts - Product Grades A And B. International Organization for Standardization, Switzerland, 2011.
[19] CEN. BS EN ISO 6892-2, metallic materials - tensile testing - part 2: method of test at elevated temperature. Brussels: European Committee for Standardization; 2011.
[20] CEN. BS EN ISO 6892-1, metallic materials - tensile testing - part 1: method of test at room temperature. Brussels: European Committee for Standardization; 2016.
[21] Tao Z, Wang XQ, Uy B. Stress-strain curves of structural and reinforcing steels after exposure to elevated temperatures. J Mater Civil Eng 2013;25:1306–16.
[22] CEN. BS EN 1993-1-2, Eurocode 3: design of steel structures - part 1-2: general rules - structural fire design. Brussels: European Committee for Standardization; 2005.
[23] Standards Australia. AS 4100, steel structures. New South Wales: Australian Building Codes Board; 1998.
[24] SAC. GB 51249, Code for fire safety of steel structures in buildings. Standardization Administration of the People's Republic of 2017 China, Beijing.
[25] AISC. ANSI/AISC 360-10, Specification for structural steel buildings. American Institute of Steel Construction, Chicago, 2010.
[26] BSI. BS 5950-8, Structural use of steelwork in building - part 8: code of practice for fire resistant design. London: British Standards Institution; 1990.
[27] Qiang X, Jiang X, Bijlaard FSK, Kolstein H. Mechanical properties and design recommendations of very high strength steel S960 in fire. Eng Struct 2016;112:60–70.
[28] Qiang X, Bijlaard F, Kolstein H. Dependence of mechanical properties of high strength steel S690 on elevated temperatures. Constr Build Mater 2012;30:73–9.
[29] Neuenschwander M, Scandella C, Knobloch M, Fontana M. Modeling elevated-temperature mechanical behavior of high and ultra-high strength steels in structural fire design. Mater Des 2017;136:81–102.
[30] Choi I, Chung K, Kim D. Thermal and mechanical properties of high-strength structural steel HSA800 at elevated temperatures. Mater Des 2014;63:544–51.
[31] Chen J, Young B, Uy B. Behavior of high strength structural steel at elevated temperatures. J Struct Eng 2006;132:1948–54.
[32] Xiong M, Liew JYR. Mechanical properties of heat-treated high tensile structural steel at elevated temperatures. Thin Wall Struct 2016;98:169–76.